

AD-A201 982

DTIC FILE COPY

4

OFFICE OF NAVAL RESEARCH

Contract N00014-80-K-0852

R&T Code _____

Technical Report No. 41

Interpretation of the Carbon Auger Line Shapes
From Adsorbed and Fragmented Ethylene on Ni (100)

By

F. L. Hutson and D. E. Ramaker

Prepared for Publication

in the

Surface Science

George Washington University
Department of Chemistry
Washington, D.C. 20052

December, 1988

Reproduction in whole or in part is permitted for
any purpose of the United States Government

This document has been approved for public release
and sale; its distribution is unlimited.

DTIC
ELECTE
DEC 19 1988
S D
H

SECURITY CLASSIFICATION OF THIS PAGE

ADA201982

REPORT DOCUMENTATION PAGE				
1a. REPORT SECURITY CLASSIFICATION Unclassified			1b. RESTRICTIVE MARKINGS	
2a. SECURITY CLASSIFICATION AUTHORITY			3. DISTRIBUTION / AVAILABILITY OF REPORT Approved for Public Release, distribution Unlimited.	
2b. DECLASSIFICATION / DOWNGRADING SCHEDULE				
4. PERFORMING ORGANIZATION REPORT NUMBER(S) Technical Report # 41			5. MONITORING ORGANIZATION REPORT NUMBER(S)	
6a. NAME OF PERFORMING ORGANIZATION Dept. of Chemistry George Washington Univ.		6b. OFFICE SYMBOL (If applicable)	7a. NAME OF MONITORING ORGANIZATION Office of Naval Research (Code 413)	
6c. ADDRESS (City, State, and ZIP Code) Washington, D.C. 20052			7b. ADDRESS (City, State, and ZIP Code) Chemistry Program 800 N. Quincy Street Arlington, VA 22217	
8a. NAME OF FUNDING / SPONSORING ORGANIZATION Office of Naval Research		8b. OFFICE SYMBOL (If applicable)	9. PROCUREMENT INSTRUMENT IDENTIFICATION NUMBER Contract N00014-80-K-0852	
6c. ADDRESS (City, State, and ZIP Code) Chemistry Program 800 North QUINCY, Arlington, VA 22217			10. SOURCE OF FUNDING NUMBERS PROGRAM ELEMENT NO. 61153 N PROJECT NO. TASK NO. PP 013-08-01 WORK UNIT ACCESSION NO NR 056-681	
11. TITLE (Include Security Classification) Interpretation of the Carbon Auger Line Shapes from Adsorbed and Fragmented Ethylene on Ni (100) (Uncl.)				
12. PERSONAL AUTHOR(S) F. L. Hutson And D. E. Ramaker				
13a. TYPE OF REPORT Interim Technical		13b. TIME COVERED FROM TO	14. DATE OF REPORT (Year, Month, Day) December 1988	15. PAGE COUNT 21
16. SUPPLEMENTARY NOTATION Prepared for Publication in Surface Science				
17. COSATI CODES FIELD GROUP SUB-GROUP			18. SUBJECT TERMS (Continue on reverse if necessary and identify by block number) Catalysis, Ethylene, Chemisorption, Auger Spectroscopy. (H) (S) (P) (Q) (R) (S) (T) (U) (V) (W) (X) (Y) (Z) (AA) (AB) (AC) (AD) (AE) (AF) (AG) (AH) (AI) (AJ) (AK) (AL) (AM) (AN) (AO) (AP) (AQ) (AR) (AS) (AT) (AU) (AV) (AW) (AX) (AY) (AZ) (BA) (BB) (BC) (BD) (BE) (BF) (BG) (BH) (BI) (BJ) (BK) (BL) (BM) (BN) (BO) (BP) (BQ) (BR) (BS) (BT) (BU) (BV) (BW) (BX) (BY) (BZ) (CA) (CB) (CC) (CD) (CE) (CF) (CG) (CH) (CI) (CJ) (CK) (CL) (CM) (CN) (CO) (CP) (CQ) (CR) (CS) (CT) (CU) (CV) (CW) (CX) (CY) (CZ) (DA) (DB) (DC) (DD) (DE) (DF) (DG) (DH) (DI) (DJ) (DK) (DL) (DM) (DN) (DO) (DP) (DQ) (DR) (DS) (DT) (DU) (DV) (DW) (DX) (DY) (DZ) (EA) (EB) (EC) (ED) (EE) (EF) (EG) (EH) (EI) (EJ) (EK) (EL) (EM) (EN) (EO) (EP) (EQ) (ER) (ES) (ET) (EU) (EV) (EW) (EX) (EY) (EZ) (FA) (FB) (FC) (FD) (FE) (FF) (FG) (FH) (FI) (FJ) (FK) (FL) (FM) (FN) (FO) (FP) (FQ) (FR) (FS) (FT) (FU) (FV) (FW) (FX) (FY) (FZ) (GA) (GB) (GC) (GD) (GE) (GF) (GG) (GH) (GI) (GJ) (GK) (GL) (GM) (GN) (GO) (GP) (GQ) (GR) (GS) (GT) (GU) (GV) (GW) (GX) (GY) (GZ) (HA) (HB) (HC) (HD) (HE) (HF) (HG) (HH) (HI) (HJ) (HK) (HL) (HM) (HN) (HO) (HP) (HQ) (HR) (HS) (HT) (HU) (HV) (HW) (HX) (HY) (HZ) (IA) (IB) (IC) (ID) (IE) (IF) (IG) (IH) (II) (IJ) (IK) (IL) (IM) (IN) (IO) (IP) (IQ) (IR) (IS) (IT) (IU) (IV) (IW) (IX) (IY) (IZ) (JA) (JB) (JC) (JD) (JE) (JF) (JG) (JH) (JI) (JJ) (JK) (JL) (JM) (JN) (JO) (JP) (JQ) (JR) (JS) (JT) (JU) (JV) (JW) (JX) (JY) (JZ) (KA) (KB) (KC) (KD) (KE) (KF) (KG) (KH) (KI) (KJ) (KK) (KL) (KM) (KN) (KO) (KP) (KQ) (KR) (KS) (KT) (KU) (KV) (KW) (KX) (KY) (KZ) (LA) (LB) (LC) (LD) (LE) (LF) (LG) (LH) (LI) (LJ) (LK) (LM) (LN) (LO) (LP) (LQ) (LR) (LS) (LT) (LU) (LV) (LW) (LX) (LY) (LZ) (MA) (MB) (MC) (MD) (ME) (MF) (MG) (MH) (MI) (MJ) (MK) (ML) (MN) (MO) (MP) (MQ) (MR) (MS) (MT) (MU) (MV) (MW) (MX) (MY) (MZ) (NA) (NB) (NC) (ND) (NE) (NF) (NG) (NH) (NI) (NJ) (NK) (NL) (NM) (NO) (NP) (NQ) (NR) (NS) (NT) (NU) (NV) (NW) (NX) (NY) (NZ) (OA) (OB) (OC) (OD) (OE) (OF) (OG) (OH) (OI) (OJ) (OK) (OL) (OM) (ON) (OO) (OP) (OQ) (OR) (OS) (OT) (OU) (OV) (OW) (OX) (OY) (OZ) (PA) (PB) (PC) (PD) (PE) (PF) (PG) (PH) (PI) (PJ) (PK) (PL) (PM) (PN) (PO) (PP) (PQ) (PR) (PS) (PT) (PU) (PV) (PW) (PX) (PY) (PZ) (QA) (QB) (QC) (QD) (QE) (QF) (QG) (QH) (QI) (QJ) (QK) (QL) (QM) (QN) (QO) (QP) (QQ) (QR) (QS) (QT) (QU) (QV) (QW) (QX) (QY) (QZ) (RA) (RB) (RC) (RD) (RE) (RF) (RG) (RH) (RI) (RJ) (RK) (RL) (RM) (RN) (RO) (RP) (RQ) (RR) (RS) (RT) (RU) (RV) (RW) (RX) (RY) (RZ) (SA) (SB) (SC) (SD) (SE) (SF) (SG) (SH) (SI) (SJ) (SK) (SL) (SM) (SN) (SO) (SP) (SQ) (SR) (SS) (ST) (SU) (SV) (SW) (SX) (SY) (SZ) (TA) (TB) (TC) (TD) (TE) (TF) (TG) (TH) (TI) (TJ) (TK) (TL) (TM) (TN) (TO) (TP) (TQ) (TR) (TS) (TT) (TU) (TV) (TW) (TX) (TY) (TZ) (UA) (UB) (UC) (UD) (UE) (UF) (UG) (UH) (UI) (UJ) (UK) (UL) (UM) (UN) (UO) (UP) (UQ) (UR) (US) (UT) (UU) (UV) (UW) (UX) (UY) (UZ) (VA) (VB) (VC) (VD) (VE) (VF) (VG) (VH) (VI) (VJ) (VK) (VL) (VM) (VN) (VO) (VP) (VQ) (VR) (VS) (VT) (VU) (VV) (VW) (VX) (VY) (VZ) (WA) (WB) (WC) (WD) (WE) (WF) (WG) (WH) (WI) (WJ) (WK) (WL) (WM) (WN) (WO) (WP) (WQ) (WR) (WS) (WT) (WU) (WV) (WW) (WX) (WY) (WZ) (XA) (XB) (XC) (XD) (XE) (XF) (XG) (XH) (XI) (XJ) (XK) (XL) (XM) (XN) (XO) (XP) (XQ) (XR) (XS) (XT) (XU) (XV) (XW) (XX) (XY) (XZ) (YA) (YB) (YC) (YD) (YE) (YF) (YG) (YH) (YI) (YJ) (YK) (YL) (YM) (YN) (YO) (YP) (YQ) (YR) (YS) (YT) (YU) (YV) (YW) (YX) (YY) (YZ) (ZA) (ZB) (ZC) (ZD) (ZE) (ZF) (ZG) (ZH) (ZI) (ZJ) (ZK) (ZL) (ZM) (ZN) (ZO) (ZP) (ZQ) (ZR) (ZS) (ZT) (ZU) (ZV) (ZW) (ZX) (ZY) (ZZ)	
19. ABSTRACT (Continue on reverse if necessary and identify by block number) The $2KVV$ Auger line shapes of ethylene on $Ni(100)$ at 100, 250, and 350 K are consistently interpreted. These line shapes are representative of π -bonded ethylene π -bonded acetylene. The Auger line shape of graphite on Ni is also interpreted. The line shapes are found to consist of adsorbate-adsorbate, adsorbate-substrate, and substrate-substrate components, which are denoted by the final location of the two holes created by the Auger process. The adsorbate-adsorbate component, for each of the molecular adsorbates, reflects the density of states of ethylene and shows negligible hole-hole correlation effects due to charge transfer from the metal. The other two components directly reflect the adsorbate-substrate π or σ bonding character and the extent of screening via charge transfer from the metal to the core excited adsorbate. and discussion Keywords:				
20. DISTRIBUTION / AVAILABILITY OF ABSTRACT <input checked="" type="checkbox"/> UNCLASSIFIED / UNLIMITED <input checked="" type="checkbox"/> SAME AS RPT. <input type="checkbox"/> DTIC USERS			21. ABSTRACT SECURITY CLASSIFICATION Unclassified	
22a. NAME OF RESPONSIBLE INDIVIDUAL Dr. David L. Nelson			22b. TELEPHONE (Include Area Code) (202) 696-4410	22c. OFFICE SYMBOL

DD FORM 1473, 84 MAR

83 APR edition may be used until exhausted.
All other editions are obsolete.SECURITY CLASSIFICATION OF THIS PAGE
Unclassified

084

1. Introduction

The formation and study of carbon and hydrocarbon species on single crystal transition metal surfaces is important to a mechanistic understanding of catalytic methanation and Fischer-Tropsch synthesis [1]. This has motivated many studies of the adsorption and decomposition of ethylene and acetylene on metal surfaces, by many different techniques, including laser induced desorption (LID), low energy electron diffraction (LEED), infra red (IR), temperature programmed desorption (TPD), Auger electron spectroscopy (AES), ultraviolet and x-ray photoelectron spectroscopy (UPS and XPS), and high resolution electron energy loss spectroscopy (HREELS) [recent works can be found in refs. 2-4]. Similar techniques have been used to study the catalytic methanation reaction, $3\text{H}_2 + \text{CO} \rightarrow \text{CH}_4 + \text{H}_2\text{O}$ [5, 6 and references therein].

Of these many techniques, AES has been particularly useful for determining the total carbon coverage [2,5,7], and also for characterizing the surface carbon (carbide or graphitic) [5,6], which appears at higher temperatures in the decomposition of hydrocarbons or methanation on the surface. AES has, however, the potential to provide much more, namely, chemical and bonding information on some of the intermediates in hydrocarbon fragments or in methanation. The C KVV Auger line shape, for example, should reflect the type of C-metal bonding (e.g. π or $\text{di-}\sigma$ bonding) of small hydrocarbons to the surface, as well as indicate something about the nature of various CH_x species. Despite all of the other techniques utilized, it remains difficult to unambiguously determine the chemical nature, the mode of bonding, and the

geometry of the adsorbed molecules, so that additional supporting information from AES might be extremely useful.

AES has not realized its full potential because of the complexity in quantitatively interpreting the various Auger line shapes, not because of the lack of AES data. Auger line shapes have been reported for several chemisorbed systems. Salmeron et al. [8] reported AES data for chemisorbed atoms (O, S, N, and C) on Cu, Ni, and Fe, and noted the presence of features due to interatomic transitions involving deexcitation of the initial adsorbate core hole from electrons in the substrate valence band. Netzer [9] reviewed the literature on AES of chemisorbed molecules as of 1981, summarizing the data for CO, NO, NH₃, C₂H₄, C₂N₂, and C₆H₆ chemisorbed on metal surfaces. He noted the presence of intermolecular features in the spectra, and the decrease in the hole-hole repulsion energies of the intramolecular features. He also indicated the need for a level of interpretation beyond the "fingerprinting" technique to understand the changes introduced by the presence of the substrate and the surface chemical bond. More recently Kamath et al. [10] reported C, N, and O KVV Auger derivative (dN(E)/dE) "fingerprints" for O₂, H₂O, CH₃OH, HCHO, CO, N₂, NH₃, CH₃NH₂, and (CH₃)₃NH chemisorbed on Ni, Cu, Pd, or Ag. Houston et al. [6] reported the "carbide" and "graphitic" Auger line shapes for the surface species arising from the reaction of CO with Ni(100) and Ni(111) at different temperatures. Most relevant to the present work, Koel [4,11] has recently presented the C KVV line shapes for C₂H₄ on Ni(100) at a temperature of 100 K and the various decomposition products at 250, 300, and 600 K. He noted that the ethylenic line shape at 100 K and carbide line shape at



First	Special
A-1	

600 K are very similar to those for ethylene and methane, respectively, except for large energy shifts [4].

Recently, we reported detailed and quantitative interpretations of the C KVV Auger line shapes of graphite [12], diamond [13], and polyethylene [14], and for the gas phase molecules, methane, ethane, ethylene, benzene, and cyclohexane [15]. These interpretations revealed the presence of satellites arising from resonant excitation, initial-state shake, and final-state shake. The principal line shape also revealed the presence of hole-hole correlation effects. These complexities make it understandable why the line shapes for the chemisorbed species were not previously interpreted in detail. However, we are now in a position to provide near quantitative interpretations of these line shapes.

We present detailed interpretations of the ethylenic, acetylenic, and graphitic C KVV Auger line shapes in this work. An interpretation of the carbidic line shapes will be published elsewhere [16]. The most significant results of this work can be summarized briefly as follows:

- 1) Although the adsorbate vs. comparable gas phase Auger line shapes exhibit some similar features, the line shapes are largely shifted in energy and are the sum of very different principal and satellite components due to screening via charge transfer from the metal.
- 2) The σ and π bonds, which bond the adsorbate to the substrate, is reflected directly in the Auger line shape of the adsorbate.

2. The ethylene vs. ethylenic line shapes.

2.a. The ethylene line shape

We have interpreted the gas-phase ethylene line shape previously [15]. The experimental KVV line shape [17], our theoretical result, and the various components are shown in Fig. 1a and summarized in Table 1. We refer to the satellite components as the ke-vve, kv-vvv, and k-vvv components, arising from resonant excitation, initial-state shake, and final-state shake, respectively. The notation here indicates the particles in the initial and final state before and after the hyphen. The "k" refers to the initial 1s core hole, the "e" to the resonantly-excited bound electron, and the "v" to a valence hole created either by the shakeoff process or by the Auger decay. We use kvv to indicate the principal or normal Auger contribution to differentiate it from the total KVV experimental line shape. We use kvv rather than k-vv to be consistent with that used historically.

The principal kvv line shape is obtained by applying the expression [15],

$$N(E) = B \sum_{ll'} [R_l R_{l'} P_{kll'} A(E + \delta_{ll'}, \Delta U_{ll'}, \rho_l \rho_{l'})]. \quad (1)$$

Here A is the Cini expression [18],

$$A(E + \delta_{ll'}, \Delta U_{ll'}, \rho_l \rho_{l'}) = \frac{\rho_l \rho_{l'}}{[1 - \Delta U_{ll'} I(E)]^2 + [\Delta U_{ll'} \pi \rho_l \rho_{l'}]^2}, \quad (2)$$

applied to the self-fold of the one-electron density of states (DOS = ρ_l),

$$\rho_l \rho_{l'} = \int \rho_l(E - \epsilon) \rho_{l'}(\epsilon) d\epsilon. \quad (3)$$

The sum is over the components ll' (i.e. the $\sigma_s \sigma_s$, $\sigma_s \sigma_p$, $\sigma_s \pi$,

σ , π , and $\pi\pi$ components). The atomic Auger matrix elements, P_{k11} , are obtained from experimental and theoretical results for neon. The relative magnitudes utilized in this work are $P_{kss} = 0.8$, $P_{ksp} = 0.5$, and $P_{kpp} = 1.0$ as reported previously [19]. $I(E)$ is the Hilbert transform of the DOS and the R_i are core hole screening factors as defined below.

In eqs. (1) and (2), ΔU is the effective final state hole-hole correlation parameter equal to the difference between the one-center and two-center repulsion integrals (i.e. $U_{11}-U_{12}$), and δ is the effective hole-hole repulsion for completely delocalized holes roaming about the entire molecule [15]. $\Delta U_{\lambda\lambda'}$, $\delta_{\lambda\lambda'}$, and the normalization constant B are obtained empirically from the best fit of eq. (1) to the experimental line shape. The subscripts $\lambda\lambda'$ on the ΔU and δ parameters are to make explicit that these parameter vary with the nature of the orbital combination; i.e. we allow just three different ΔU 's and δ 's, namely for the $\sigma\sigma$, $\sigma\pi$, and $\pi\pi$ contributions.

We have shown previously [20] that in covalent systems, intermediate levels of localization can occur. The holes may localize from a molecular orbital to a "cluster" orbital, or further to a bond orbital. A simple examination of the MO's for the alkenes suggests strongly that the appropriate local orbital is the planar arrangement of three sp^2 bond orbitals about a single carbon atom for the σ bands, and a single p orbital for the π bands [15]. In light of the above, the ΔU 's can be interpreted in this work as the difference between the hole-hole repulsion when two holes are localized on the same local (cluster or atomic) orbital

verses when they are localized on different neighboring local orbitals.

The DOS for ethylene was obtained empirically from x-ray emission (XES) [21] and XPS [22] data in a procedure described previously [15]. Briefly the XES spectra reflect the σ , and π DOS, the XPS spectra reflect primarily the σ , DOS (actually $\sigma + (1/14)(\sigma + \pi)$) [23]. The DOS components were weighted to provide an electronic configuration of $\sigma, \sigma, 1, 1, \pi, 1, 1$.

The factors R_l in eq.(1) are to make our theory consistent with the previously derived final state rule for Auger line shapes [24]. The final state rule indicates that 1) the shape of the individual $1l'$ contributions should reflect the DOS in the final state, and 2) the intensity of each $1l'$ contribution should reflect the electron configuration of the initial state [24]. For the kvv line shape, the final state is without the core hole. We assume that the DOS in the final state and ground state are similar, so the spectral shape should reflect the ground DOS. However, the initial state in the kvv process has a core hole, therefore the relative intensities should reflect the electron configuration of the initial-core-hole (CHS) state. The R_l factors are defined,

$$R_l = \int \rho_{CHS,l}(e) de / \int \rho_l(e) de,$$

to include this effect. In systems where a single l component dominates the core screening, such as in the chemisorbed species, these R_l factors can significantly alter the total line shape. In ethylene, all l components change similarly, so that the R_l factors can be ignored [15].

A resonant Auger satellite arises when Auger decay occurs in the presence of a localized electron, which can be created by

resonant excitation into an excitonic or bound state upon creation of the core hole [25]. The excited electron can either be a spectator to the Auger decay or participate in it, producing the ke-vve or ke-v contributions, respectively.

The resonant line shapes can be obtained from the one-electron DOS. The spectator case has a two-hole final state so that a self-fold of the DOS is appropriate. Correlation effects can again be introduced by utilizing the Cini expression. However, the spectator electron can screen the two holes and reduce the hole-hole repulsion. In this work we assume correlation effects are negligible in the ke-vve satellite so that its line shape is given simply by the DOS self-fold [15]. The ke-v satellite has just one final state hole, so its line shape is given accurately by the one-electron DOS. Like for the kvv line shape, energy shifts to higher binding energy are again required [15]. δ_{ke-vve} is approximately equal to $U_v - U_k$ and δ_{ke-v} to $E_0 + U_k$. Here U_k and U_v are equal to the core- (or valence-) hole, excited-electron attraction energy, and E_0 is the excited-electron binding energy in the absence of the core hole. $E_0 + U_k$ is the binding energy in the presence of the core hole.

Initial-state shake, kv-vvv, satellites arise when Auger decay occurs in the presence of a localized valence hole, which was created via the shake-off process during the initial ionization [26]. We have determined previously that the line shape for the kv-vve satellite in alkenes can be approximated by a self-fold of the DOS, but with twice the ΔU and δ parameters [15].

Final-state shake, k-vvv, satellites arise when Auger decay occurs simultaneously with shakeoff of a valence hole [26]. The

energy required for the shakeoff process decreases the kinetic energy of the Auger electron, so that the k-vvv satellite appears as a rather structureless contribution over a wide range of energies near the bottom of the total line shape. We have utilized [15] a function due to Bethe to approximate this lineshape. In general, one can expect approximately the same amount of final-state as initial-state shake, so that these two satellite contributions should have comparable intensity [15].

Table 1 summarizes the results found previously for ethylene [15]. Note that the kvv principal component accounts for only about half of the total KVV line shape. The kv-vve and k-vvv shakeoff satellites have almost equal intensity, which is about equal to the probability for shakeoff. The δ 's for the kvv contribution are relatively large, around 10 eV. δ_{k-vvv} is reduced to 3 eV due to the screening of the π^* electron as indicated above. δ_{k-v} , which as indicated above should be equal to the binding energy of the π^* orbital in the presence of a core hole, is 7 eV, consistent with that indicated by core-hole absorption spectra [15].

2.b The ethylenic line shape

The chemisorption of ethylene at low temperatures is molecular for most metal surfaces. HREELS of molecular ethylene have been reported for Pt(111), Pd(111), Pd(100), Rh(111), Ag(110), Ru(100), Cu(100), Fe(110), Fe(111), Ni(111), Ni(110), and Ni(5(111)x(100)) (see refs. 1-11 in [3]), as well as for Ni(100) [2,3]. The molecule is believed to lie bonded with the C=C bond parallel to the surface for all but Ni(111) and Fe(110) [3]. It has been shown

that ethylene chemisorbed over Cu(100), Ag(110) and Ni(100) at lower temperatures retains most of its π character, adsorption over most of the other surfaces is accompanied by rehybridization and di- σ bonding to the substrate [3]. Multiple scattering X α calculations [27] for ethylene on Ni(100), modeled by a 10-atom Ni cluster, reveals that charge donation occurs from the C₂H₄ π orbital to a Ni σ_{pi} orbital, and corresponding back-donation of charge into the C₂H₄ π^* orbital. The Ni levels near the Fermi energy are virtually unaffected, the valence σ orbitals appear to uniformly shift to higher binding energy by about 1.5 eV, the π orbital remains nearly unshifted [27].

The above indicates that the Auger line shape reported by Koel [11] for ethylene chemisorbed on Ni(100) at 100K (see Fig. 1) corresponds to that for π -bonded molecular ethylene. The Auger data reported by Koel was x-ray excited to reduce beam damage effects. The line shape given in Fig. 1 results after a linear background has been subtracted, and an inelastic and elastic backscattered spectrum has been deconvoluted from the raw data [4,11]. Details of this normal Auger data treatment have been given several times before [28]. This deconvolution procedure is necessary to remove the large secondary electron and extrinsic-loss contributions which appear in any line shape taken from a solid. This data treatment is not necessary for line shapes taken from gases [15]. The similarity in spectral line shape between the extrinsic and intrinsic (i.e. the k-vvv process) loss contributions means that all of the k-vvv satellite contribution is unavoidably removed from an experimental KVV line shape for the solid.

We will model the ethylenic one-electron DOS by using the DOS obtained previously [15] for gas phase ethylene. We will include the Auger contributions arising because of the partial electron occupation of the π^* orbital in the chemisorbed state by including separate VV, $V\pi^*$, and $\pi^*\pi^*$ contributions, where V indicates collectively the normally occupied valence orbitals.

The VV contribution should be directly relatable to that utilized for gas phase ethylene. However, a major difference arises because, in the final state, charge transfer from the substrate into the π^* orbital occurs to screen the two or three holes left by the Auger or shakeoff-Auger process. This charge transfer into the π^* orbital is known to occur for CO and NO chemisorbed on metals [29], and it has been indicated earlier for other unsaturated [30] and even saturated [31] molecules. This charge transfer has the effect of decreasing the ΔU and δ parameters; the transferred charge playing the role of the resonantly excited electron in the gas phase as reflected in the resonant satellite. Indeed, the line shape for the principal kvv contribution to the VV component should be similar to the ke-vve line shape for ethylene, i.e. a DOS self-fold with $\Delta U = 0$.

Resonant satellites do not appear in the VV contribution because Keol excited it with Mg K α non-resonant x-rays [11]. However the $V^*\pi^*$ contribution should be similar to the ke-v contribution for ethylene gas since both should reflect the one-electron ethylene DOS. We must fold the ethylene DOS, ρ_{gas} , with the π^* DOS. In the LCAO-MO approximation, the π^* orbital mixes with much of the Ni 3d valence band [32], indeed the hole left by the Auger decay involving the π^* orbital probably ends up in the

Ni. Therefore we fold ρ with the Ni 3d DOS as obtained from band calculations [33], and as indicated in Fig. 2a.

Finally as mentioned above, Salmeron et al. [8] and Netzer [9] have noted the presence of "inter" -atomic or -molecular features near the top of most Auger line shapes of chemisorbed line shapes. These are again probably facilitated through an intra-atomic $\pi^*\pi^*$ Auger process, but which ultimately appears inter-atomic in character because both holes end up on the substrate. Thus we model the $\pi^*\pi^*$ line shape by utilizing the Ni L₂VV Auger line shape [34]. This line shape reflects a self-fold of the d-DOS, but with significant correlation effects consistent with the Cini-expression [35]. The Ni L₂VV line shape is shown in Fig. 2b on a two-hole binding energy scale relative to the vacuum. This was obtained from the experimental kinetic energy scale utilizing an L₂ binding energy of 855 eV and a work function of 5 eV [35]. This line shape was utilized unshifted for the VV component in Fig. 1b.

Each of the three components (i.e. the VV, $V\pi^*$, $\pi^*\pi^*$ components) will also have a kv-vvv satellite contribution. The kv-vvv satellite contribution to VV should be similar to the kvv contribution in ethylene gas (i.e. the kve-vvve line shape in the chemisorbed molecule should be similar to the kvv line shape in the gas). The kv-vvv line shapes for the $V\pi^*$ and $\pi^*\pi^*$ components were assumed to be the same as the principal kvv contributions. A constant energy shift (i.e. 14 eV) to higher binding energy to account for the larger repulsion of the 3 final state holes in the kv-vvv process was included for all three components. The kv-vvv satellite was fixed at 20% of the kvv contribution for all three components. The energy shift and the 20% relative intensity of the

kv-vvv satellite was determined to give optimal agreement with experiment. A final-state shake k-vvv satellite contribution does not exist in the ethylenic line shape because it has been subtracted out in the background and deconvolution processes as mentioned above.

Table 1 summarizes the individual components. The total theoretical line shape was generated by a linear least squares fit of the three (i.e. the VV, $V\pi^*$, $\pi^*\pi^*$) components to experiment. Fig. 1b shows each component and compares the total theoretical line shape with the experimental one. The agreement between theory and experiment is good; all features present in the experimental line shape appear also in the theory with nearly the same energy and relative intensity, except for the feature around 26 eV which is a little too large in the theory. This is comparable to the peak at around 40 eV in ethylene gas (see Fig. 1a) where the theory is similarly too large. In the gas phase, this over-estimate was attributed to the absence of multiplet effects in the theory. This may also be the problem for chemisorbed ethylene, although these effects are expected to be reduced because of the screening charge transfer from the substrate.

The relative intensities of the four components can be understood within the final state rule, as defined above. The electronic configuration per carbon atom in the ground state of the chemisorbed ethylene, assuming charge neutrality, is nominally $\sigma^2\pi^1-\pi^*\pi^*$, where the x indicates the π bonding and π^* back-bonding charge transfer involved in the interaction with the metal substrate. Upon creation of the core hole, we assume the valence electronic configuration, again assuming charge neutrality, becomes

$\sigma^* \pi^* \pi^*$ or $V^* \pi^*$, where y is the net charge transfer in the presence of the initial core hole. The relative intensities of the components, $VV: V\pi^*: \pi^* \pi^*$ should then be $16:8y:y^2$, or upon including the P_{ii} matrix elements $13:7y:y^2$. Best agreement with the results obtained from the fit to the experimental lineshapes as reported in Table 1 is obtained when $y=1.3$, which gives relative intensities of 55:38:7 (total normalized to 100) compared to 56:34:10 in Table 1. The 1.3 total electron transfer is consistent with the 1.3 core hole screening electrons found in benzene as determined from ab-initio theoretical calculations [12].

3. The "acetylenic" line shapes

The line shapes for ethylene at 250 and 300 K, obtained by Koel[11] and shown in Fig. 3, are different from those at 100 K, suggesting either decomposition of the ethylene or at least rearrangement on the surface. HRERLS [2,3] data indicates that just below 250 K, C_2H_4 decomposes into $C_2H_2 + H_2$, the C_2H_2 existing as di- σ bonded acetylene on the surface of Ni(100). This still leaves the basic ethylene backbone (i.e. one C-C π bond); however, now two σ adsorbate-substrate (C-M) bonds are involved instead of a single π C-M bond as at 100 K. Thus we anticipate that the Auger line shape is composed of three components as above, only now we label them the VV , $V\sigma$, and $\sigma\sigma$ components. The VV component is exactly as that found above, but the $\sigma\sigma$ component should be different from the $\pi^* \pi^*$ component.

We approximate the C-M σ bonding DOS by utilizing the DOS for transition metal carbides, in this case that for C chemisorbed on Ni. The approximate carbidic DOS can be obtained from two

different sources. Rozei et al. [36] obtained UPS data for carbidic overlayers obtained by heating a Ni (111) surface at 200-250 °C in CO. The difference between the UPS ($h\nu \approx 35$ eV) spectra for the clean and carburized (0.3 ML carbon) Ni surface is given in Fig. 2c. This difference spectrum is compared with the LCAO-MO calculated DOS obtained by Feibelman [37] for a (1x1) overlayer of C atoms on an 11-layer Ru(0001) film. The calculated results indicate that the narrow feature near the Fermi level in both the empirical and calculated "DOS" is due predominantly to a non-bonding p_z -orbital. The broad feature between 2 and 8 eV arises primarily from the bonding p_x, p_y orbitals, and the feature around 11 eV arises mainly from the s orbitals. Reasonable agreement between the empirical and theoretical DOS is found except for the "s" feature. It is sharp and around 11 eV in the calculated DOS, very broad and centered at 15 eV in the empirical DOS. The slow tailing off of the empirical "s" feature may be an artifact of the subtraction procedure, but more likely it is due to the presence of π -CH carbene species which are also known to reside on the surface [16]. The carbene species are expected to have the "s" feature at significantly higher binding energy, thus explaining the tailing off of the "s" feature in the Rozei data. Comparison of self-folds with the experimental carbidic Auger line shape [16] suggests that the s DOS should peak around 13 eV. For the work to be described below, we will utilize the theoretical DOS, but with the s feature shifted to 13 eV binding energy.

The self-folds of the theoretical and empirical DOS are indicated in Fig. 2d. The self-fold of the theoretical DOS was Gaussian broadened by 2 eV. Comparison of the σ and π^* C-M bonding

DOS and the $\pi^*\pi^*$ and $\sigma\sigma$ kvv components, as we have approximated them, indicates very significant differences exist between these two chemisorption bonds. Although the dominant feature in both components falls at 14-16 eV, the $\sigma\sigma$ component has significant contributions down to 40 eV, whereas the $\pi^*\pi^*$ contribution extends down to only 20 eV. The large differences in the DOS means that the cross-folds (i.e. the $V\sigma$ and $V\pi^*$) will also be different. These differences in the component line shapes, and differences in the relative intensities of each component, we believe are the reasons for the differences in the total Auger line shapes at 100 and 250 K.

We wish to emphasize the basic differences between the σ and π adsorbate-substrate bonds as we believe they are reflected in the Auger line shapes. The weak π bond does not significantly alter the Ni DOS, as suggested by MS-X α calculations [27], thus it only provides a means for the charge transfer so that the final state Auger holes may end up on the substrate Ni atom nearest the ethylene. Our utilization of the Ni DOS and $L_{2,3}VV$ line shape above reflects this assumption. On the other hand, the stronger σ C-M bonds do alter the Ni DOS, and we assume a carbidic C-M bond character. Our utilization of the carbidic DOS and self-folds reflects this assumption.

Our previous studies [38] of the metal-carbide C KVV Auger line shapes [39,40] have indicated that the hole-hole correlation effects decrease as the heat of formation of the metal carbides decreases. Since Ni_3C is thermally unstable (i.e. has a negative heat of formation), the Ni_3C Auger line shape should have little or no correlation effects [41-43], and this is consistent with our

findings [16]. Therefore we approximate the three components to the 250 K Auger line shape by simple folds of the appropriate DOS. The kv-vvv contributions to the components are approximated also by simple folds, however consistent with the 100 K spectrum, the kv-vvv contributions were shifted to 14 eV higher binding energy to account for the hole-hole repulsion of the 3-hole final state. The relative intensity of the kv-vvv to kvv components was varied, but best agreement with experiment was found at 20 %, consistent with that found for the 100 K spectrum.

The optimal fit of the 3 components, VV, V σ , and $\sigma\sigma$, is shown in Fig. 3a, the relative intensities and description of each component is given in Table 1. The $\sigma\sigma$ component was shifted 2 eV toward the Fermi level to provide better agreement with experiment. A similar shift was required to give optimal agreement for the carbide line shapes [16]. This shift simply suggests that the carbide DOS utilized to approximate the $\sigma\sigma$ component must be shifted by 1 eV to better approximate the C-M DOS in chemisorbed systems. Reasonably good agreement is found in Fig. 3a ; however, not as good as found for the 100 K spectrum shown in Fig. 1b. This may result from the deconvolution process, which is the most uncertain near the bottom of the spectrum, where most of the disagreement lies. Alternately, it may result from a breakdown in our approximation for reasons to be described below.

Comparison of the VV:V σ : $\sigma\sigma$ relative intensities to that found for VV:V π^* : $\pi^*\pi^*$ above reveals a significantly greater substrate-substrate contribution in the 250 K spectrum. This is to be expected in the intimately σ bonded adsorbate at 250 K, because even in the ground state some C-M charge transfer occurs.

Quantitatively, the relative $VV:V\sigma:\sigma\sigma$ component intensities (28:49:23) suggest an electron configuration per carbon atom in the core hole state of around $(C-C,H)^2(C-M)^{1.5}$. The notation here indicates that each C atom has 3 electrons shared in C-C and C-H bond orbitals and 2.5 electrons in the C-M bond orbitals. Since the agreement between the theoretical and experimental line shapes in Fig. 3a is not real good, a considerable uncertainty exist in the relative component intensities, and thus in the electronic configuration above. Nevertheless, this electronic configuration is plausible if one makes the reasonable assumption that 1 electron is shared in each of the C-C, 2 C-H, and C-M bonds in the ground state, and that 1.5 additional electrons transfer from the substrate into the C-M bond orbitals in the presence of a C core hole. The magnitude of this charge transfer is slightly greater than the 1.3 electrons found for π bonded ethylene above, and is consistent with the more intimate σ bond to acetylene. However, we cannot be sure that this difference is significant because of uncertainties in the component intensities here.

The Auger spectrum reported by Koel [11] at 300 K (Fig. 3b) is different again from that found at 250 K. HREELS data suggests partial decomposition to a carbene species (CH), and perhaps also to acetylide ($-C_2H$), in this temperature region [2,3]. Further heating to 600 K gives yet a different spectrum, which we show elsewhere [16] is due to $\equiv CH$ on the surface. If the formation of acetylide is negligible, then the 300 K spectrum should be a sum of the line shapes for CH and di- σ bonded acetylene ($-CH_2=CH_2-$). We test this by fitting the experimental 250 and 600 K spectra to the 300 K spectra. Fig 3b shows an excellent fit. Table I shows that

the relative intensities are 35% CH and 65% $-\text{CH}_2=\text{CH}_2-$. This indicates that the formation of acetylide is indeed negligible at 300K, or that the acetylide Auger lineshape can be approximated as a linear combination of the lineshapes for $\equiv\text{CH}$ and $-\text{CH}_2=\text{CH}_2-$. The latter is unlikely, since acetylide ($-\text{C}\equiv\text{C}-\text{H}$) has $\text{C}\equiv\text{C}$ character, while $-\text{CH}_2=\text{CH}_2-$ has $\text{C}=\text{C}$ character.

4. Graphite

Fig. 4 compares the C Auger line shapes for bulk graphite [12] and graphite chemisorbed on the surface of Ni(111) [6]. The chemisorbed graphite spectrum was obtained from CO/Ni(111) heated to 650 K [6]. A similar spectrum is obtained upon heating $\text{C}_2\text{H}_2/\text{Ni}(100)$ above 650 K [11]. Both the bulk and chemisorbed spectra result after background removal and deconvolution of the loss features as described by Houston et al. [6].

The differences in the two graphite spectra can be attributed to the charge transfer from the substrate to the carbon atom with the Auger initial-state core-hole just as for ethylene above. We again fit three components to the chemisorbed spectra, namely the VV , $\text{V}\pi^*$, and $\pi^*\pi^*$ components. We assume the VV component line shape is the same as that for bulk graphite. The $\text{V}\pi^*$ component is obtained from a fold of the graphite DOS with the Ni DOS, and the $\pi^*\pi^*$ component line shape is assumed to be the same as the Ni $\text{L}_{2,3}\text{VV}$ line shape, just as assumed above for ethylene/Ni at 100 K. Table 1 summarizes the components, and Fig. 4 shows the optimal fit to the experimental spectrum. The fit is good except for the region around 10 eV.

The relative component intensities, $\text{VV}:\text{V}\pi^*:\pi^*\pi^* = 85:11:4$ can again be used to calculate the charge transfer from the Ni

substrate in the presence of a carbon core hole. We can use the expression derived above for ethylene, namely $13:7y:y^2$. Unfortunately, the relative component intensities above do not provide a consistent value for the charge transfer, y , as they did for ethylene. The ratio $V\pi^*:VV$ gives $y \approx 0.24$, while the $\pi^*\pi^*:VV$ ratio gives $y \approx 0.78$. However, the relative intensity of the $\pi^*\pi^*$ component is very uncertain because around 10 eV, where the $\pi^*\pi^*$ component dominates, the theoretical and experimental line shapes are in poor agreement. Therefore, we accept the 0.24 electron transfer. This is considerably less than for ethylene. We attribute this decreased charge transfer in graphite to the greater intra-adsorbate π electron screening expected in a fully developed two-dimensional monolayer of graphite [12]. The decreased substrate screening also accounts for the lack of a significant change in the VV component line shape from the bulk line shape. We have shown previously that the bulk line shape contains significant correlation effects, with ΔU of the order of 4 eV in the $\sigma\sigma$ components [12]. Apparently on the surface of Ni, no significant change in ΔU occurs.

5. Discussion and Summary

Comparison of the results summarized in Table 1 and Figs. 1-4 reveals some interesting points. First, note the trend in the optimum shakeoff intensity, $kV-vvv/kVv$, found for ethylene vs. that for the chemisorbed molecules (37% vs. 20%). This intensity ratio is a direct measure of the probability for the shakeoff "hole" to remain on the atom with the initial core hole to "witness" the Auger decay. It is smaller for the adsorbate, obviously because

the shakeoff "hole" has a significant probability for escape through the adsorbate-substrate bond (i.e. electron transfer from the substrate). Escape before the Auger decay results in a normal kVV contribution. In bulk graphite, no $kV-VVV$ satellite appears at all, because the shakeoff hole does not remain on the atom with the initial core hole, but propagates throughout the graphite [12]. This is still true in the graphitic over layer.

The second point concerns the correlation effects as indicated by the ΔU parameter. In the π -bonded ethylene case, ΔU is zero for the kVV contribution to the VV and $V\pi^*$ components, but not for the $\pi^*\pi^*$ component, since in the experimental $L_{2,3}VV$ Auger line shape utilized for $\pi^*\pi^*$, ΔU is known to be around 2.5 eV [34]. This may appear inconsistent at first. However, ΔU is very dependent on the spatial arrangement of the two final state holes. The $4sp$ valence electrons cannot effectively screen two holes in the relatively local d orbitals on a single Ni atom (U_{11}). Holes on two different Ni atoms (U_{12}) are easily screened. Hence the effective ΔU ($= U_{11} - U_{12}$) in bulk Ni, or in this case for the $\pi^*\pi^*$ component, is significant. In chemisorbed ethylene, the two holes on a single C sp^2 cluster orbital are apparently easily screened by the π and π^* electrons in the adsorbate, hence ΔU is negligible in the VV component. Likewise, ΔU is expected to be small in the $V\pi^*$ component. For di- σ bonded acetylene, ΔU is found to be negligible for all three components. Here ΔU is zero for the $\sigma\sigma$ component, because two holes in the more delocalized C-M σ bonds are easily screened by the Ni metallic electrons [38]. ΔU is zero for the VV and $V\sigma$ components just as for chemisorbed ethylene.

The correlation effects in the graphitic overlayer are also

very interesting. The VV component is the same as for bulk graphite, where large correlation effects are present. We suggested previously [15] that this probably arises because of a decrease of U_{11} by screening, leaving ΔU relatively large. The small charge transfer from the Ni substrate does not change this in the overlayer. However, the poor agreement around 10 eV between the theoretical and experimental lineshapes for the graphitic overlayer suggests that our approximation of the $\pi^*\pi^*$ component by the $L_{2,3}VV$ Ni lineshape is not a very good one, although it was fine for chemisorbed ethylene. Fig. 4 suggests that better agreement would have been obtained if we had utilized a simple fold of the Ni one-electron DOS, which would have peaked much closer to the Fermi level. This suggests a most interesting "reverse" (graphite to Ni) screening process; i.e. when both holes end up on the Ni substrate, the graphitic overlayer apparently causes ΔU to be less than for pure Ni. Although the diffuse Ni s valence electrons cannot effectively screen two localized d holes, the electrons in the graphitic π and π^* orbitals, which are intimately bonded with the surface Ni d orbitals, apparently can effectively screen these two d holes.

We have also indicated previously that the δ for the kvv contribution reflects the repulsion of two holes delocalized about the entire molecule, but that the δ for the kv-vvv contribution reflects the repulsion of holes localized on a methyl-like cluster orbital. This is consistent with the data in Table 2. Upon chemisorption of the ethylene, the δ for the kvv contribution reduces from 9 eV to 0. The electron transferred from the metal obviously screens very effectively the two holes delocalized about

the molecule. However, the δ for the $kv-vvv$ contribution decreases from 18 eV to just 14 eV. As one might expect, the transferred electron cannot effectively screen the two holes localized on a single methyl-like cluster orbital.

Finally, we should point out a significant difference in character between the gas phase and chemisorbed hydrocarbon Auger line shapes. In the gas phase, the C-C and C-H bonds are all similar in nature, so that delocalized molecular orbitals are formed, which are characterized by the global symmetry of the molecule. However, the Auger line shape reflects only the self-fold of the DOS, which obscures all but the gross features of these DOS. Thus, the comparable alkanes and alkenes have very similar DOS self-folds (e.g. those for ethane vs. ethylene, cyclohexane vs. benzene, and graphite vs. diamond are surprisingly similar). The experimental line shapes do reflect significant differences however. We have shown that this arises because of the different correlation effects in the $\sigma\sigma$ vs. the $\pi\pi$ contributions (i.e. ΔU is around 2 eV in the $\sigma\sigma$ contributions and 0 in the $\pi\pi$ contributions). But, on the surface, all hole-hole correlation effects are effectively removed because of the charge transfer from the metal, so that the experimental line shapes now do reflect primarily the DOS self-fold. But now the bonds are not all similar, since the C-H and C-C bonds are very different in character from the C-M (metal substrate) bonds. In this case some molecular orbitals (MO's) are localized primarily on the molecular adsorbate, and some on the C-M adsorbate-substrate bond. Thus the experimental line shape clearly has regions at higher two-hole binding energy which reflect the intramolecular MO's and those at lower binding energy which reflect

the C-M MO's. Furthermore, we have shown that the self-fold of the intramolecular MO's can be approximated by the DOS self-fold of the gas phase molecules at least for the case of the weakly π bonded ethylene. In the case of the di- σ bonded acetylene, the experimental line shape does not agree with the theoretical lineshape as well as we might have hoped. This may result from a breakdown in this approximation.

In summary, we have consistently interpreted four different C KVV Auger line shapes, namely that for ethylene/Ni(100) at 100, 250, and 300 K, and for graphite on Ni(111). We have shown that the intra-adsorbate (VV) components reflect the DOS of the gas phase molecule, or the bulk solid in the case of graphite, so that the chemisorption bond can be treated independently from the intra-adsorbate contributions. For ethylene, intra-adsorbate correlation effects are reduced to zero because of charge transfer from the substrate, so that the various contributions to the line shape are significantly differently than for the gas phase. This in fact makes the Auger line shape for the adsorbate more directly reflect the molecular DOS than for the gas phase. In graphite, no significant reduction of the correlation effects is seen on the surface so that the VV component of the chemisorbed line shape and the bulk line shape are the same.

Significant adsorbate-substrate Auger components ($V\pi^*$ and $\pi^*\pi^*$ or $V\sigma$ and $\sigma\sigma$) are evident. These directly reflect the σ or π chemisorption bond character. The extent of charge transfer from the metal to the adsorbate, in the presence of a core hole, is seen directly from the intensities of these components, as well as from the changes in the VV component line shapes.

We suggest that Auger spectroscopy can be used to find valuable information about chemisorbed systems, and that it can be effectively used with other spectroscopies in the study of catalytic reactions and Fischer-Tropsch synthesis.

Acknowledgments: The authors would like to thank B. E. Koel for making his experimental Auger data available before publication. This work was supported in part by the Office of Naval Research.

Table 1

Summary of components comprising the theoretical Auger line shapes.

Component	Basic Character ^a	ΔU^b (eV)	δ^c (eV)	Intensity ^d
<u>C₂H₄ gas</u>				
VV: kvv	$p_{\text{eth}}^*p_{\text{eth}}$	ΔU^e	$\delta^f(9)$	54
kv-vvv	"	$2\Delta U^e$	$2\delta^f(18)$	20
k-vvv	Bethe	-	-	15
ke-vve	$p_{\text{eth}}^*p_{\text{eth}}$	0	3	13
ke-v	p_{eth}	-	7	2
<u>C₂H₄/Ni(100) at 100 K: π bonded ethylene</u>				
VV: kvv	$p_{\text{eth}}^*p_{\text{eth}}$	0	0	45 } 56
kv-vvv	"	ΔU^e	$\delta+5(14)^g$	11 }
V π^h : kvv	$p_{\text{eth}}^*p_{\pi}$	0	0	27 } 34
kv-vvv	"	0	14	7 }
$\pi^h\pi^h$: kvv	Ni L ₂₃ VV	2.5 ^h	0	8 } 10
kv-vvv	"	2.5 ^h	14	2 }
<u>C₂H₄/Ni(100) at 250 K: di-σ bonded acetylene</u>				
VV: kvv	$p_{\text{eth}}^*p_{\text{eth}}$	0	0	22 } 28
kv-vvv	"	0	14	6 }
V σ : kvv	$p_{\text{eth}}^*p_{\text{carb}}$	0	0	39 } 49
kv-vvv	"	0	14	10 }
$\sigma\sigma$: kvv	$p_{\text{carb}}^*p_{\text{carb}}$	0	-2 ⁱ	18 } 23
kv-vvv	"	0	12 ⁱ	5 }
<u>C₂H₄/Ni(100) at 300K</u>				
C ₂ H ₄ /Ni at 250K: di- σ acetylene		-	-	65
C ₂ H ₄ /Ni at 600K: carbene (CH)		-	-	35
<u>CO,H₂/Ni(111) at 650K: graphitic</u>				
VV: kvv	bulk C KVV	ΔU^j	0	85
kv-vvv	-	-	-	0
V π^k : kvv	$p_{\text{graph}}^*p_{\pi}$	0	0	11
kv-vvv	-	-	-	0
$\pi^k\pi^k$: kvv	Ni L ₂₃ VV	2.5 ^k	0	4
kv-vvv	-	-	-	0

*This column indicates the basic source of the component line shapes, such as a fold (ρ^*p) of the indicated density of states (the DOS of either gas phase ethylene, bulk Ni, Ni₂C, or bulk graphite), the experimental Auger lineshapes (the Ni L_{2,3}VV or bulk graphite C KVV), or the theoretical Bethe line shape as described in Ref. (15)

*The effective hole-hole correlation parameter in eq. (2).

*The effective de-localized hole-hole repulsion parameter in eq. (2).

*Relative intensity normalized to 100

*Signifies values of 2 eV for the $\sigma\sigma$ orbitals, 1 eV for the $\sigma\pi$, and 0 for the $\pi\pi$.

*Signifies values of 9 eV for the $\sigma\sigma$ and 11 eV for the $\sigma\pi$ and $\pi\pi$ orbitals. The 9 eV is indicated in parentheses above.

*Signifies values indicated in f above plus 5 eV, providing a values of 14 eV for the $\sigma\sigma$ orbitals.

*Although the experimental Ni L_{2,3}VV Auger lineshape was utilized, the effective ΔU has been shown to be around 2.5 eV, see Ref. 35.

*The $\sigma\sigma$ component was moved 2 eV closer to the Fermi level for optimal alignment; see text.

*Although the experimental C KVV Bulk graphite Auger lineshape was utilized, the effective ΔU 's have been shown (Ref. 15) to be the same as for gas phase ethylene, which are indicated in e above.

*As indicated in h above, the effective ΔU in the experimental Ni L_{2,3}VV lineshape is 2.5 eV; however, Fig. 4 suggests that it should be much smaller. In the text, we attribute this indicated decrease to reverse (i.e. graphite to Ni) electron screening in the Auger final state.

References

1. V. Ponec, in *Catalysis*, Vol 5. Eds. G.C. Bond and G. Webb, Specialist Periodical Reports, (The Chemical Society, London, 1982), p. 48.
2. S. Akhter and J.M. White, *Surf. Sci.* 180 (1987) 19.
3. F. Zaera and R.B. Hall, *Surf. Sci.* 180 (1987) 1.
4. B.E. Koel and D.L. Neiman, *Chem. Phys. Lett.* 130 (1986) 164.
5. D.W. Goodman, R.D. Kelly, T.E. Madey, and J.T. Yates, Jr., *J. Catalysis* 63 (1980) 226.
6. J.E. Houston, D.E. Peebles, and D.W. Goodman, *J. Vac. Sci. Technol. A1* (1983) 995.
7. B.E. Koel, J.M. White, D.W. Goodman, *Chem. Phys. Lett.* 88 (1982) 236.
8. M. Salmeron and A.M. Baro, *Surf. Sci.* 49 (1975) 356; M. Salmeron, A.M. Baro, and J.M. Rojo, *Phys. Rev. B13* (1976) 4348.
9. F.P. Netzer, *Appl. Surf. Sci.* 7 (1981) 289.
10. P. V. Kamath, K. Prabhakaran, and C.N.R. Rao, *Indian J. Phys.* 60B (1986) 84.
11. B.E. Koel, private communication.
12. J.E. Houston, J.W. Rogers, R.R. Rye, F.L. Hutson, and D.E. Ramaker, *Phys. Rev. B34* (1986) 1215.
13. D.E. Ramaker and F.L. Hutson, *Solid State Commun.* 63 (1987) 335.
14. F.L. Hutson and D.E. Ramaker, *Phys. Rev. B35* (1987) 9799.
15. F.L. Hutson and D.E. Ramaker, *J. Chem. Phys.* 87 (1987) 6824.
16. F.L. Hutson and D.E. Ramaker, to be published
17. R.R. Rye, T.E. Madey, J.E. Houston, and P.H. Holloway, *J. Chem. Phys.* 69 (1978) 1504; *Ind. Eng. Chem. Prod. Res. Dev.* 18 (1979) 2; R.R. Rye, D.R. Jennison, and J.E. Houston, *J. Chem. Phys.* 73 (1980) 4867.
18. M. Cini, *Solid State Commun.* 20 (1976) 655; *Phys. Rev. B17* (1978) 2788; G.A. Sawatzky, *Phys. Rev. Lett.* 39 (1977) 504.

19. F.L. Hutson, D.E. Ramaker, B.I. Dunlap, J.D. Ganjei, and J.S. Murday, *J. Chem. Phys.* 76 (1982) 2181.
20. B.I. Dunlap, F.L. Hutson, and D.E. Ramaker, *J. Vac. Sci. Technol.* 18 (1981) 556.
21. R.A. Mattson and R.C. Ehlert, *J. Chem. Phys.* 48 (1968) 5465.
22. K. Siegbahn et al. "ESCA Applied to Free Molecules" (North Holland Publ. Co., New York, 1969), p. 103.
23. J.S. Murday, B.I. Dunlap, F.L. Hutson, and P. Oelhafen, *Phys. Rev.* B24 (1981) 4764.
24. D.E. Ramaker, *Phys. Rev.* B25 (1982) 7341.
25. This process is also referred to as autoionization or resonant photoemission: see for example E. Bertel, R. Stockbauer, and T.E. Madey, *Surf. Sci.* 141 (1984) 355.
26. E.J. McGuire, *Phys. Rev.* A11 (1975) 1880.
27. I.A. Howard and G. Dresselhaus, *Surf. Sci.* 130 (1984) 229.
28. D.E. Ramaker, J.S. Murday, and N.H. Turner, *J. Electron Spectrosc. Related Phenom.* 17 (1970) 45.
29. G.D. Stucky, R.R. Rye, D.R. Jennison, and J.A. Kelber, *J. Am. Chem. Soc.* 104 (1982) 5951; B.E. Koel, J.M. White, and G.M. Loubriel, *J. Chem. Phys.* 77 (1982) 2665.
30. D.R. Jennison, J.A. Kelber, and R.R. Rye, *Chem. Phys. Lett.* 77 (1981) 694.
31. K. Hermann and P.S. Bagus, *Phys. Rev.* 28 (1983) 560.
32. D.B. Kang and A.B. Anderson, *Surf. Sci.* 155 (1985) 639.
33. C.S. Wang and J. Callaway, *Phys. Rev.* B15 (1977) 298.
34. G.G. Kleiman, *Appl. Surf. Sci.* 11/12 (1982) 730.
35. T. Jach and C.J. Powell, *Phys. Rev. Lett.* 46 (1981) 953.
36. R. Rosei, S. Modesti, F. Sette, C. Quaresima, A. Savoia, and P. Perfetti, *Phys. Rev.* B29 (1984) 3416.
37. P.J. Feibelman, *Phys. Rev.* B26 (1982) 5347; F.J. Himpsel, K. Christmann, P. Heimann, and D.E. Eastman, P.J. Feibelman, *Surf. Sci.* 115 (1982) L159.
38. P.E. Pehrsson and D.E. Ramaker, *J. Vac. Sci. Technol.* A3 (1985) 1315; and to be published.

39. G.R. Gruzalski, D.M. Zehner, and G.W. Ownby, Surf. Sci. Lett. 157 (1985) L395.
40. J.M. Schulga and G.L. Gutsev, J. Electron. Spectrosc. Related Phenom. 34 (1984) 39.
41. J.P. Coad and J.C. Riviere, Surf. Sci. 25 (1971) 609.
42. S. Sinharoy, M.A. Smith, and L.L. Levenson, Surf. Sci. 72 (1978) 710; J. Vac. Sci. Technol. 14 (1977) 475.
43. J. Kleefeld and L.L. Levenson, Thin Solid Films 64 (1979) 389.

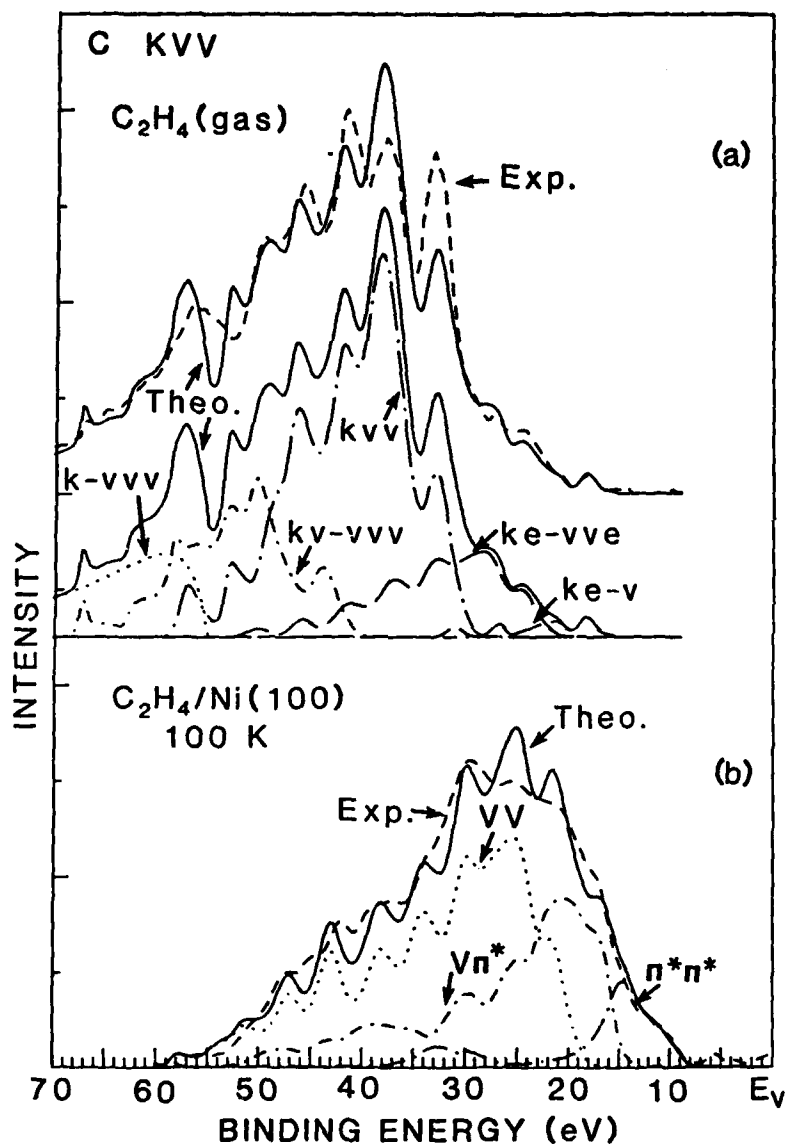
Figure Captions

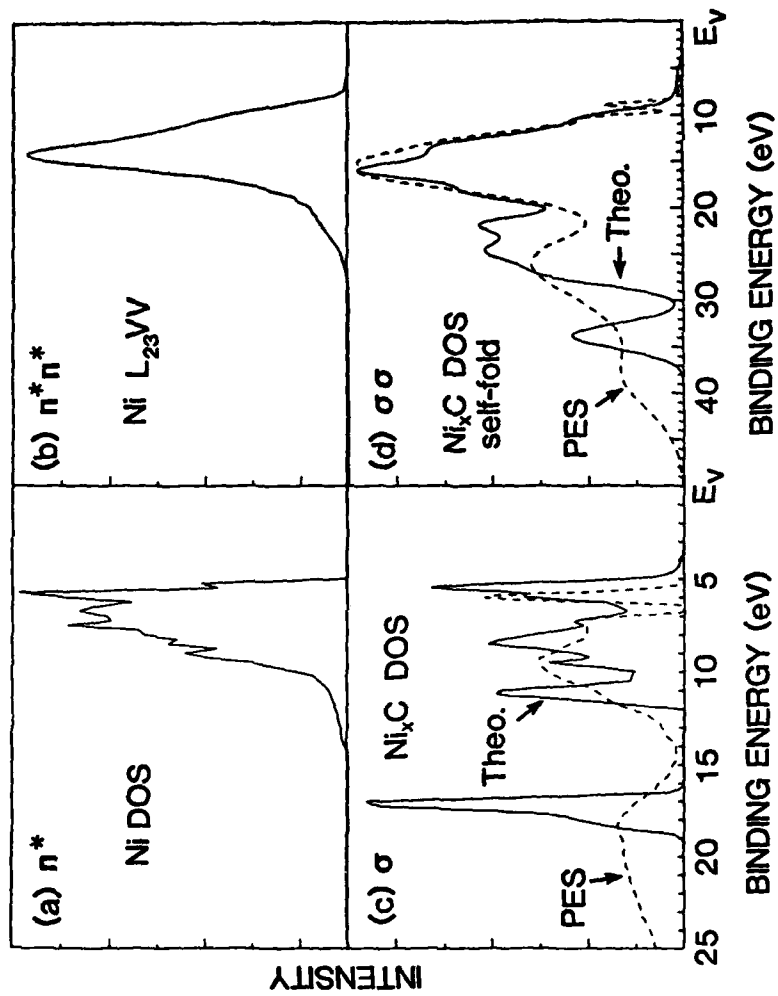
- Fig. 1**
- a) Comparison of the C KVV experimental and theoretical Auger line shapes for ethylene gas as reported previously [15]. The various contributions (kvv, kv-vvv, k-vvv, ke-v, ke-avv) were obtained as described in the text and in ref. 15, and are summarized in Table 1.
 - b) Comparison of the experimental and theoretical Auger line shapes for ethylene chemisorbed on Ni(100) at 100 K (π -bonded ethylene). The experimental data was obtained by Koel [11]. The three component (VV, $V\pi^*$, $\pi^*\pi^*$) line shapes were obtained as described in the text and summarized in Table 1. The relative intensities were obtained by least squares fit to the experimental data.
- Fig. 2**
- a) The calculated Ni bulk density of states as obtained from ref. 33 and utilized here to represent the π^* adsorbate-substrate DOS
 - b) The experimental $L_{2,3}VV$ Auger lineshape of Ni metal [34,35] (i.e. the $\pi^*\pi^*$ component).
 - c) Comparison of the empirical Ni carbide DOS as obtained by Rozel [36] from photoemission data and by Feibelman [37] from theory as described in the text, and utilized here to represent the σ adsorbate-substrate DOS.
 - d) The self-folds of the empirical and theoretical carbide DOS (i.e. the $\sigma\sigma$ component). The self-fold of the theoretical DOS was Gaussian broadened by 2 eV.
- Fig. 3**
- a) Comparison of the experimental [11] and theoretical Auger line shapes for ethylene on Ni(100) at 250 eV (di- σ

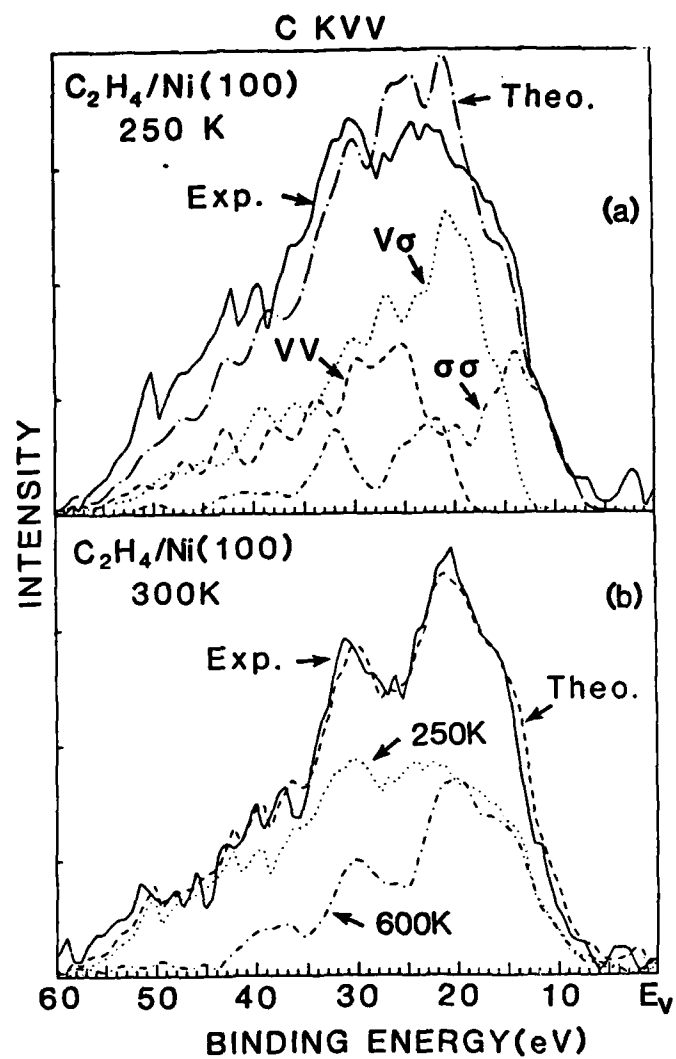
bonded acetylene). The three component (VV , $V\sigma$, $\sigma\sigma$) line shapes were obtained as described in the text and summarized in Table 1. The relative intensities were obtained by least squares fit to the experimental data.

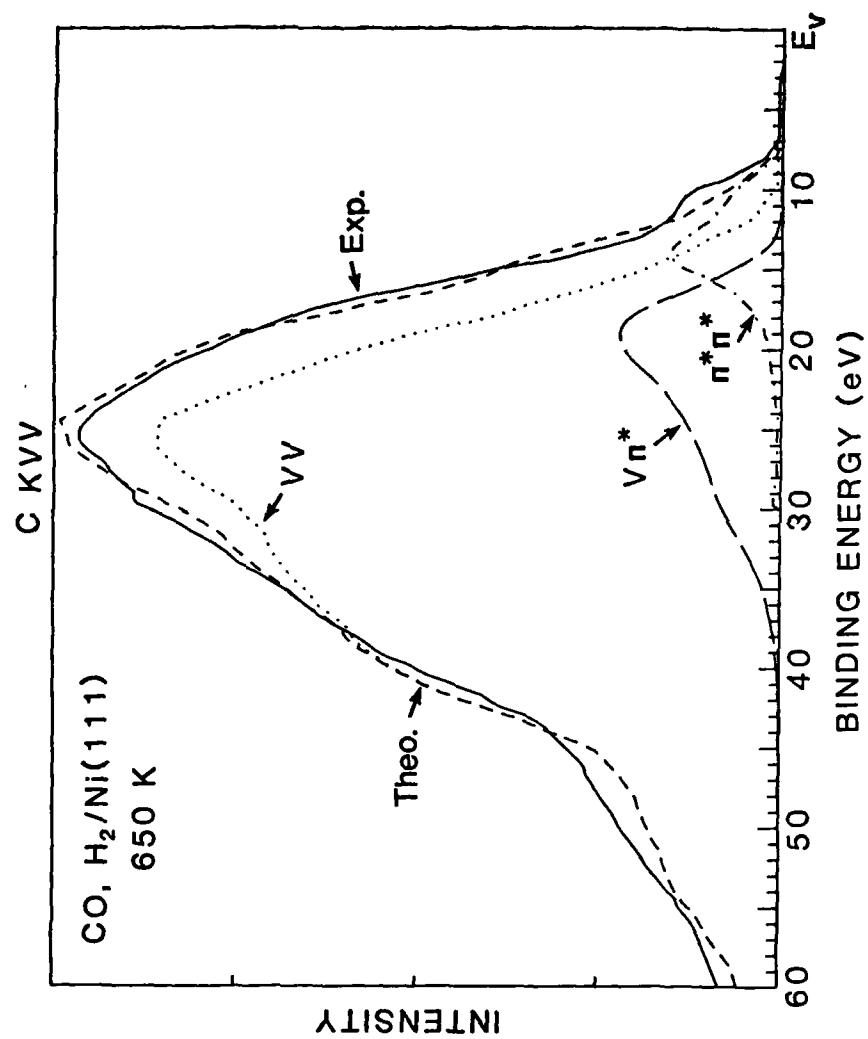
b) Same as the above except for ethylene on Ni(100) at 300 K. The two components are the experimental line shapes obtained at 250 K (di- σ bonded acetylene) and at 600 K (CH).

Fig. 4. Comparison of the experimental [6] and theoretical Auger line shapes for chemisorbed graphite on Ni(111). The component (VV , $V\pi^*$, and $\pi^*\pi^*$) line shapes were obtained as described in the text and summarized in Table 1. The relative intensities were obtained by least squares fit to the experimental line shape.









ABSTRACTS DISTRIBUTION LIST, 056/625/629

Dr. G. A. Somorjai
Department of Chemistry
University of California
Berkeley, California 94720

Dr. J. Murday
Naval Research Laboratory
Code 6170
Washington, D.C. 20375-5000

Dr. W. T. Peria
Electrical Engineering Department
University of Minnesota
Minneapolis, Minnesota 55455

Dr. Keith H. Johnson
Department of Metallurgy and
Materials Science
Massachusetts Institute of Technology
Cambridge, Massachusetts 02139

Dr. S. Sibener
Department of Chemistry
James Franck Institute
5640 Ellis Avenue
Chicago, Illinois 60637

Dr. Arold Green
Quantum Surface Dynamics Branch
Code 3817
Naval Weapons Center
China Lake, California 93555

Dr. A. Wold
Department of Chemistry
Brown University
Providence, Rhode Island 02912

Dr. S. L. Bernasek
Department of Chemistry
Princeton University
Princeton, New Jersey 08544

Dr. W. Kohn
Department of Physics
University of California, San Diego
La Jolla, California 92037

Dr. Stephen D. Kevan
Physics Department
University Of Oregon
Eugene, Oregon 97403

Dr. David M. Walba
Department of Chemistry
University of Colorado
Boulder, CO 80309-0215

Dr. L. Kesmodel
Department of Physics
Indiana University
Bloomington, Indiana 47403

Dr. K. C. Janda
University of Pittsburg
Chemistry Building
Pittsburg, PA 15260

Dr. E. A. Irene
Department of Chemistry
University of North Carolina
Chapel Hill, North Carolina 27514

Dr. Adam Heller
Bell Laboratories
Murray Hill, New Jersey 07974

Dr. Martin Fleischmann
Department of Chemistry
University of Southampton
Southampton SO9 5NH
UNITED KINGDOM

Dr. H. Tachikawa
Chemistry Department
Jackson State University
Jackson, Mississippi 39217

Dr. John W. Wilkins
Cornell University
Laboratory of Atomic and
Solid State Physics
Ithaca, New York 14853

Dr. Ronald Lee
R301
Naval Surface Weapons Center
White Oak
Silver Spring, Maryland 20910

Dr. Robert Gomer
Department of Chemistry
James Franck Institute
5640 Ellis Avenue
Chicago, Illinois 60637

Dr. Horia Metiu
Chemistry Department
University of California
Santa Barbara, California 93106

Dr. W. Goddard
Department of Chemistry and Chemical
Engineering
California Institute of Technology
Pasadena, California 91125

DL/1113/87/2

ABSTRACTS DISTRIBUTION LIST, 056/625/629

Dr. J. E. Jensen
Hughes Research Laboratory
3011 Malibu Canyon Road -
Malibu, California 90265

Dr. J. H. Weaver
Department of Chemical Engineering
and Materials Science
University of Minnesota
Minneapolis, Minnesota 55455

Dr. A. Reisman
Microelectronics Center of North Carolina
Research Triangle Park, North Carolina
27709

Dr. M. Grunze
Laboratory for Surface Science
and Technology
University of Maine
Orono, Maine 04469

Dr. J. Butler
Naval Research Laboratory
Code 6115
Washington D.C. 20375-5000

Dr. L. Interante
Chemistry Department
Rensselaer Polytechnic Institute
Troy, New York 12181

Dr. Irvin Heard
Chemistry and Physics Department
Lincoln University
Lincoln University, Pennsylvania 19352

Dr. K. J. Klaubunde
Department of Chemistry
Kansas State University
Manhattan, Kansas 66506

Dr. C. B. Harris
Department of Chemistry
University of California
Berkeley, California 94720

Dr. R. Bruce King
Department of Chemistry
University of Georgia
Athens, Georgia 30602

Dr. R. Reeves
Chemistry Department
Rensselaer Polytechnic Institute
Troy, New York 12181

Dr. Steven M. George
Stanford University
Department of Chemistry
Stanford, CA 94305

Dr. Mark Johnson
Yale University
Department of Chemistry
New Haven, CT 06511-8118

Dr. W. Knauer
Hughes Research Laboratory
3011 Malibu Canyon Road
Malibu, California 90265

Dr. Theodore E. Madey
Surface Chemistry Section
Department of Commerce
National Bureau of Standards
Washington, D.C. 20234

Dr. J. E. Demuth
IBM Corporation
Thomas J. Watson Research Center
P.O. Box 218
Yorktown Heights, New York 10598

Dr. M. G. Lagally
Department of Metallurgical
and Mining Engineering
University of Wisconsin
Madison, Wisconsin 53706

Dr. R. P. Van Duyne
Chemistry Department
Northwestern University
Evanston, Illinois 60637

Dr. J. M. White
Department of Chemistry
University of Texas
Austin, Texas 78712

Dr. Richard J. Saykally
Department of Chemistry
University of California
Berkeley, California 94720

ABSTRACTS DISTRIBUTION LIST, 056/625/629

Dr. F. Carter
Code 6170
Naval Research Laboratory
Washington, D.C. 20375-5000

Dr. Richard Colton
Code 6170
Naval Research Laboratory
Washington, D.C. 20375-5000

Dr. Dan Pierce
National Bureau of Standards
Optical Physics Division
Washington, D.C. 20234

Dr. R. G. Wallis
Department of Physics
University of California
Irvine, California 92664

Dr. D. Ramaker
Chemistry Department
George Washington University
Washington, D.C. 20052

Dr. J. C. Hemminger
Chemistry Department
University of California
Irvine, California 92717

Dr. T. F. George
Chemistry Department
University of Rochester
Rochester, New York 14627

Dr. G. Rubloff
IBM
Thomas J. Watson Research Center
P.O. Box 218
Yorktown Heights, New York 10598

Dr. J. Baldeschwieler
Department of Chemistry and
Chemical Engineering
California Institute of Technology
Pasadena, California 91125

Dr. Galen D. Stucky
Chemistry Department
University of California
Santa Barbara, CA 93106

Dr. A. Steckl
Department of Electrical and
Systems Engineering
Rensselaer Polytechnic Institute
Troy, New York 12181

Dr. John T. Yates
Department of Chemistry
University of Pittsburgh
Pittsburgh, Pennsylvania 15260

Dr. R. Stanley Williams
Department of Chemistry
University of California
Los Angeles, California 90024

Dr. R. P. Messmer
Materials Characterization Lab.
General Electric Company
Schenectady, New York 12217

Dr. J. T. Keiser
Department of Chemistry
University of Richmond
Richmond, Virginia 23173

Dr. R. W. Plummer
Department of Physics
University of Pennsylvania
Philadelphia, Pennsylvania 19104

Dr. E. Yeager
Department of Chemistry
Case Western Reserve University
Cleveland, Ohio 44106

Dr. N. Winograd
Department of Chemistry
Pennsylvania State University
University Park, Pennsylvania 16802

Dr. Roald Hoffmann
Department of Chemistry
Cornell University
Ithaca, New York 14853

Dr. Robert L. Whetten
Department of Chemistry
University of California
Los Angeles, CA 90024

Dr. Daniel M. Neumark
Department of Chemistry
University of California
Berkeley, CA 94720

Dr. G. H. Morrison
Department of Chemistry
Cornell University
Ithaca, New York 14853

DL/1113/87/2

TECHNICAL REPORT DISTRIBUTION LIST, GEN

	<u>No. Copies</u>		<u>No. Copies</u>
Office of Naval Research Attn: Code 1113 800 N. Quincy Street Arlington, Virginia 22217-5000	2	Dr. David Young Code 334 NORDA NSTL, Mississippi 39529	1
Dr. Bernard Douda Naval Weapons Support Center Code 50C Crane, Indiana 47522-5050	1	Naval Weapons Center Attn: Dr. Ron Atkins Chemistry Division China Lake, California 93555	1
Naval Civil Engineering Laboratory Attn: Dr. R. W. Drisko, Code L52 Port Hueneme, California 93401	1	Scientific Advisor Commandant of the Marine Corps Code RD-1 Washington, D.C. 20380	1
Defense Technical Information Center Building 5, Cameron Station Alexandria, Virginia 22314	12 high quality	U.S. Army Research Office Attn: CRD-AA-IP P.O. Box 12211 Research Triangle Park, NC 27709	1
DTNSRDC Attn: Dr. H. Singerman Applied Chemistry Division Annapolis, Maryland 21401	1	Mr. John Boyle Materials Branch Naval Ship Engineering Center Philadelphia, Pennsylvania 19112	1
Dr. William Tolles Superintendent Chemistry Division, Code 6100 Naval Research Laboratory Washington, D.C. 20375-5000	1	Naval Ocean Systems Center Attn: Dr. S. Yamamoto Marine Sciences Division San Diego, California 92132	1